

The examination of power MOSFET voltage and current waveforms during switching transitions reveals that the device characterization now practiced by industry is inadequate. In this Note, device waveforms are explained by considering the interaction of a vertical JFET driven in cascode from a lateral MOSFET in combination with the interelectrode capacitances. Particular attention is given to the drain-voltage waveform and its dual-slope nature. The three terminal capacitances now published by the industry are shown to be valid only for zero drain current. For cases where the gate drive is a voltage step generator with internal fixed resistance, the drain voltage characteristics are inferred from the gate current drive behavior and compared to observed waveforms. The nature of the "asymmetric switching times" is explained.

A waveform family is proposed as a more descriptive and accurate method of characterization. This new format is a plot of drain voltage and gate voltage versus normalized time. A family of curves is presented for a constant load resistance with  $V_{DS}$  varied. Gate drive during switching transitions is a constant current with voltage compliance limits of 0 and 10 volts. Time is normalized by the value of gate driving current. The normalization shows excellent agreement with data over five orders of magnitude, and is bounded on one extreme by gate propagation effects and on the other by transition time self-heating (typically tens of nanoseconds to hundreds of microseconds).

### Device Models

The keystone of an understanding of power MOSFET switching performance is the realization that the active device is bimodal and must be described using a model that accounts for the dual nature. Buried in today's power MOSFET devices is the equivalent of a depletion layer JFET that contributes significantly to switching speed. Figure 1 is a cross-sectional view of a typical power MOSFET, with MOSFET/JFET symbols superimposed on the structure.

Figure 2 is obtained by taking the lateral MOS and vertical JFET from this conception and adding all the possible node-to-node capacitances. Computed values of the six capacitances for a typical device structure suggest that device behavior may be adequately modeled using only three capacitors in the manner of Figure 3. This is the model to be employed for analysis and study.

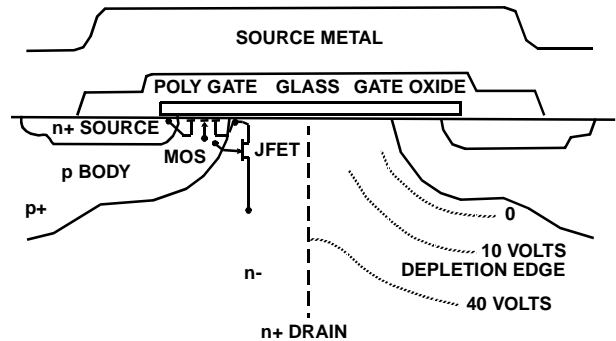


FIGURE 1. CROSS-SECTION VIEW OF MOSFET SHOWING EQUIVALENT MOS TRANSISTOR AND JFET

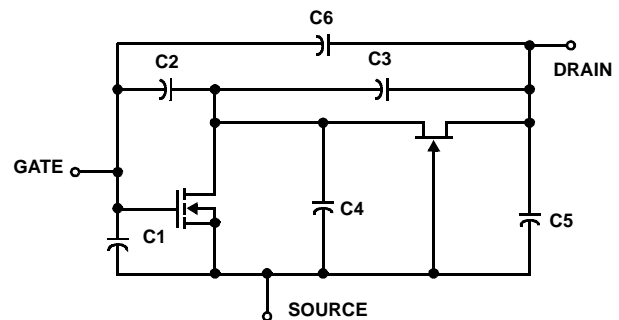


FIGURE 2. MOS TRANSISTOR WITH CASCODE-CONNECTED JFET AND ALL CAPACITORS

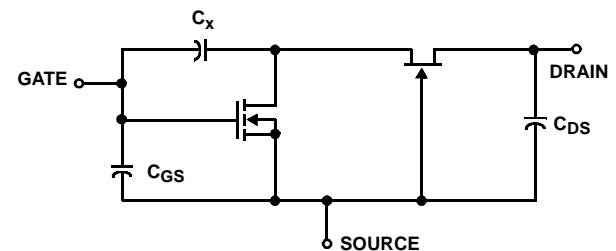


FIGURE 3. FIGURE 2 SIMPLIFIED

### Gate Drive: Constant Voltage or Constant Current

Before moving on to the study of the equivalent circuit states of the model, a gate-drive forcing function which is easy to represent, relates to reality, and best illustrates device behavior must be chosen. The choice may be immediately narrowed to two:

- (1) An instantaneous step voltage with internal resistance  $R$ , Figure 5.
- (2) An instantaneous step current with infinite internal resistance, Figure 6.



## State 2: MOS Active, JFET Active

This state graphically illustrates the dramatic influence that the JFET has on the power MOSFET drain-voltage waveform. Instead of having to discharge  $C_X$  from  $V_{DD}$  to ground, the lateral MOSFET need only swing  $V_X$  to ground, a much smaller voltage thanks to the grounded gate JFET. Since the interaction of  $R_L$  with the device capacitances has a second-order effect on the drain voltage, the equivalent circuit of Figure 7 predicts a drain voltage change of:

$$dV_G/dt = g_M R_L I_G / [C_{GS} + C_X(1 + g_M/g_{MJ})]$$

In all but the smallest power-MOSFET devices,  $C_X$  is several thousand picofarads and  $g_M/g_{MJ}$  is of the order of 3:1. Power-MOSFET devices exhibit a high  $dV_D/dt$  switching rate because of the cascode-connected JFET, not because  $C_{RSS}$  ( $C_{RSS} = C_{GD}$ ) is a small value, as zero-drain-current data sheet capacitance values might lead one to believe. If  $C_{RSS}$  were, in actuality, small, long drain voltage tails would not exist. The tail response is a direct result of JFET saturation. In order to delineate the transition from state 2 to state 3, a drain voltage at which the transition occurs must be defined.  $V_{DK}$  is the knee voltage at which linear extrapolations of drain-voltage slopes intersect. The time duration of state 2 is:

$$t_2(t_6) = (V_{DD} - V_{DK})[C_{GS} + C_X(1 + g_M/g_{MJ})]/g_M R_L I_G$$

## State 3: MOS Active, JFET Saturated

When the JFET saturates, the  $g_{MJ}V_X$  current generator becomes a short circuit and the equivalent circuit predicts:

$$dV_D/dt = g_M R_L I_G / [C_{GS} + C_X(1 + g_M R_L)]$$

This is the Miller effect so often referred to in older texts that describe the behavior of grounded-cathode vacuum-tube amplifier circuits. Allowing for the fact that  $1 + g_M R_L$  is approximately equal to  $g_M R_L$  and  $C_X(1 + g_M R_L)$  is very much larger than  $C_{GS}$ , the expression for drain-voltage tail time is:

$$t_3(t_5) = (V_{DK} - V_{D(SAT)})C_X/I_G$$

## State 4: MOS Saturated, JFET Saturated (Turn-Off)

In this state, in addition to  $g_{MJ}V_X$  being shorted, the  $g_M V_G$  current generator is shorted, and  $I_G$  is occupied with charging  $C_X$  and  $C_{GS}$ , in parallel, from the peak value of  $V_G$  to  $V_{G(SAT)}$ . The time required for this is:

$$t_4 = (V_G - V_{G(SAT)})(C_{GS} + C_X)/I_G$$

Since a value for  $C_{GS}$  may be measured independently of switching time, the method described is the simplest way of determining  $C_X$ .

On turn-off, the state time equations are equally applicable, but in reverse order (states 5 and 6); see the idealized waveform of Figure 4.

## Experimental Verification

The four switching states just analyzed indicate that for a given device, all four switching state times are inversely proportional to the magnitude of the gate drive current. Figure 8 illustrates the switching performance of a typical power MOSFET across three decades of gate drive current and time. In each case the data slope is almost a perfect -1.

## A New Device Characterization

Figure 8 could not be a reasonable device data sheet presentation because it does not give the designer any information on a typical value for  $C_X$ , nor does it convey how  $V_{DK}$ ,  $g_M$ ,  $g_M/g_{MJ}$ , and  $V_{G(sat)}$  vary with drain current. What would be of enormous value to the designer is a plot of  $V_D(t)$ ,  $V_G(t)$  for selected values of  $V_{DD}$  and  $I_D$  within device ratings.

A reasonable characterization would be as follows:

1. The x axis would be normalized in terms of gate current drive.
2. The y axis would be normalized in terms of percent maximum rated  $BV_{DSS}$  (0 to 100%).
3.  $R_L = BV_{DSS}/I_{D(max)}$  would define the drain load resistance.
4. Four plots of  $V_D(t)$ ,  $V_G(t)$  at 100%, 75%, 50%, and 25%  $BV_{DSS(max)}$  would be shown.

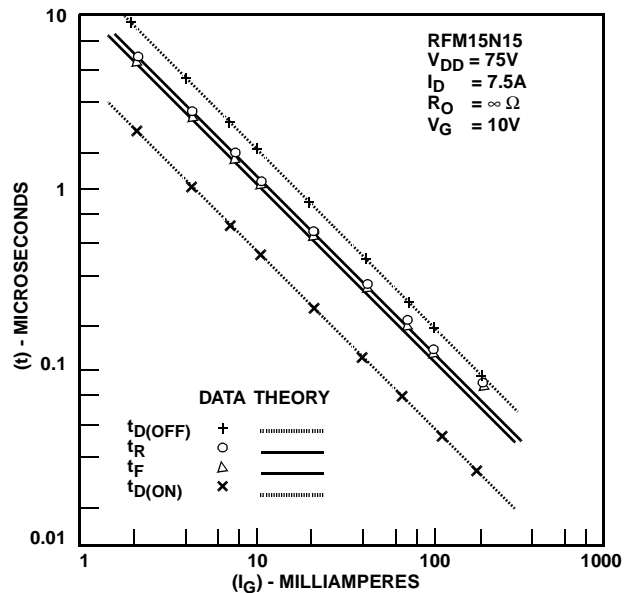


**FIGURE 8. CONSTANT GATE CURRENT SWITCHING TIME**

Figure 9 is such a plot for the RFM15N15 power MOSFET. With such a plot, a designer can estimate device switching performance under any resistive gate/drain conditions.

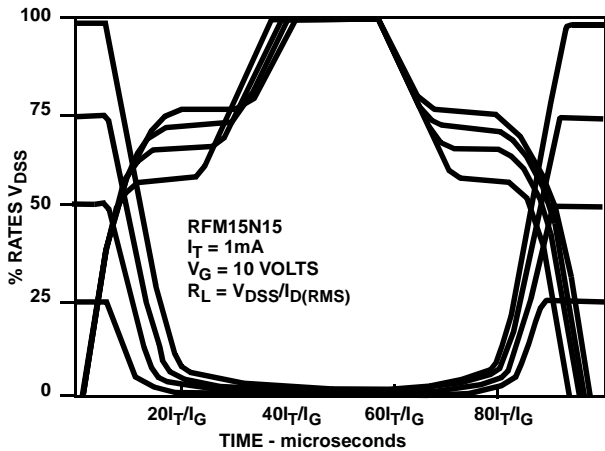


FIGURE 9. NORMALIZED RFM15N15 SWITCHING WAVEFORMS FOR CONSTANT GATE-CURRENT DRIVE.

### Step-Voltage Gate Drive

The majority of power MOSFET applications employ a step gate-voltage input with a finite source resistance  $R_O$ . Often  $R_O$  for turn-on is not the same as  $R_O$  for turn-off. How can switching times for these situations be estimated using the switching characterization curves just described? The analy-

sis for resistive step voltage inputs, which is complex because the gate current is no longer constrained to be constant, but is a function of device gate-voltage response, is covered in Appendix A. (A second, shorter appendix, B, has been added to illustrate the estimation of  $R_O$  for some practical gate drive circuits.) Table 1 summarizes the common switching equations, and indicates the appropriate  $I_G$  to be used in each state for relating step voltage drives to the characterization curves.

### Experimental Verification

Since the switching equations for step currents and voltages differ only by gate-current magnitudes for the same device type, one would expect a plot of switching time versus  $1/R_O$  to be of the same form as those obtained for a step current drive. This is exactly the case, as Figure 10 is merely a variation of Figure 8. Using the relationships of Table 1, the observed differences between Figures 7 and 9 can be pinpointed. The two sets of experimental curves confirm that, on the basis of the short-circuit drive current  $V_G/R_O$  equaling the constant  $I_G$ ,  $t_{D(on)}$ ,  $t_R$ ,  $t_{D(off)}$ , and  $t_F$  will all be longer, as predicted by the ratios of the gate drive currents of Table 1. Notice also that  $t_R$ ,  $t_F$  switching symmetry is disrupted by the use of a step voltage with source resistance  $R_O$ . For states 2 and 6 the time ratio is:

TABLE 1. COMMON SWITCHING EQUATIONS

	CONSTANT CURRENT	STATE 1: MOS OFF, JFET OFF	CONSTANT VOLTAGE
TURN ON	$t = \frac{C_{ISS} V_{GS(TH)}}{I_G}$		$t = R_O C_{ISS} \ln \frac{[1]}{[1 - V_{GS(TH)}/V_G]}$
	$I_G = I_T$	STATE 2: ACTIVE, ACTIVE	$I_G = (V_G - V_{GS(TH)})/R_O$
		$t = \frac{[V_{DD} - V_{DK}] [C_{GS} + C_X (1 + g_M/g_{MJ})]}{g_M R_L I_G}$	
	$I_G = I_T$	STATE 3: ACTIVE, SATURATED	$I_G = (V_G - V_{G(SAT)})/R_O$
		$t = \frac{(V_{DK} - V_{D(SAT)})C_X}{I_G}$	
TURN OFF	$I_G = I_T$	STATE 4: SATURATED, SATURATED	$I_G = -V_G/R_O$
	$t = \frac{(C_{GS} + C_X)(V_G - V_{G(SAT)})}{I_G}$		$t = R_O(C_{GS} + C_X) \ln (V_G/V_{G(SAT)})$
	$I_G = I_T$	STATE 5: ACTIVE, SATURATED	$I_G = (V_G - V_{G(SAT)})/R_O$
		$t = \frac{(V_{DK} - V_{D(SAT)})C_X}{I_G}$	
	$I_G = I_T$	STATE 6: ACTIVE, ACTIVE	$I_G = (V_G - V_{G(SAT)})/R_O$
	$t = \frac{[V_{DD} - V_{DK}] [C_{GS} + C_X (1 + g_M/g_{MJ})]}{g_M R_L I_G}$		

**Experimental Verification**

Since the switching equations for step currents and voltages differ only by gate-current magnitudes for the same device type, one would expect a plot of switching time versus  $1/R_O$  to be of the same form as those obtained for a step current drive. This is exactly the case, as Figure 10 is merely a variation of Figure 8. Using the relationships of Table 1, the observed differences between Figures 7 and 9 can be pinpointed. The two sets of experimental curves confirm that, on the basis of the short-circuit drive current  $V_G/R_O$  equaling the constant  $I_G$ ,  $t_D(\text{on})$ ,  $t_R$ ,  $t_D(\text{off})$ , and  $t_F$  will all be longer, as predicted by the ratios of the gate drive currents of Table 1. Notice also that  $t_R$ ,  $t_F$  switching symmetry is disrupted by the use of a step voltage with source resistance  $R_O$ . For states 2 and 6 the time ratio is:

$$\frac{t_{\text{TURN-ON}}}{t_{\text{TURN-OFF}}} = \frac{V_G(\text{SAT})}{V_G - V_{GS(\text{TH})}}$$

For states 3 and 5 the time ratio is:

$$\frac{t_{\text{TURN-ON}}}{t_{\text{TURN-OFF}}} = \frac{V_G(\text{SAT})}{V_G - V_G(\text{SAT})}$$

Utilization of available maximum gate drive voltage and current can be optimized for fastest power MOSFET switching speed through the use of constant-current gate drive at the expense of increased gate-drive circuit complexity.

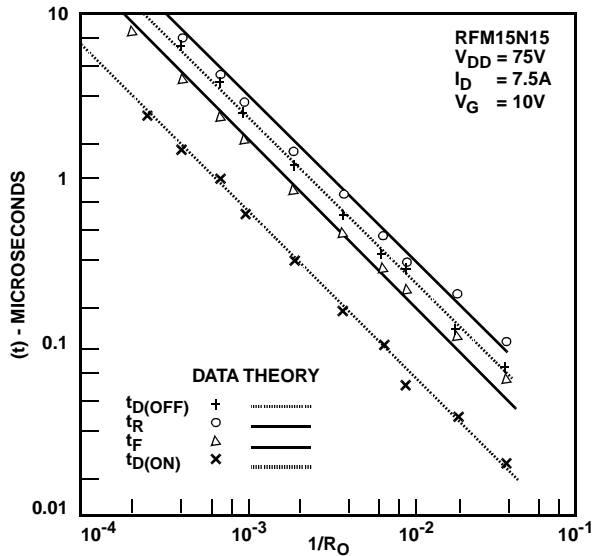


FIGURE 10. CONSTANT GATE VOLTAGE SWITCHING TIME

**Using the Characterization Curve, Figure 9**

To estimate the switching times for an RFM15N15 power MOSFET under the conditions  $V_G = 10\text{V}$ ,  $V_{DD} = 75\text{V}$ ,  $R_O = 100\text{ ohms}$ , and  $R_L = 10\text{ ohms}$ , precedes as follows:

**State 1: MOS Off, JFET Off**

This time can be estimated without recourse to the curves

$$t = 100(1200 \times 10^{-12}) \ln [1/(1 - 4/10)]$$

$$t = 61 \text{ ns}$$

**State 2 & 6: MOS Active, JFET Active**

$$I_G = (10 - 4)/100 = 60\text{mA}$$

$$t = \frac{(\text{curve divisions}) \times I_T \mu\text{s}}{60} = \frac{9}{60} = 150\text{ns}$$

**State 3: MOS Active, JFET Saturated**

$$I_G = (10 - 7)/100 = 30\text{mA}$$

$$t = \frac{(\text{curve divisions}) \times I_T \mu\text{s}}{30} = \frac{14}{30} = 467\text{ns}$$

**State 4: MOS Saturated, JFET Saturated**

$$C_{GS} + C_x = (\text{gate voltage slope})(\text{test current})$$

$$= (1.5 \times 10^{-6}\text{s/5 volts})(10\text{mA})$$

$$= 3000\text{pF}$$

$$t = 100(3000 \times 10^{-12}) \ln [10/6.6]$$

$$t = 125\text{ns}$$

**State 5: MOS Active, JFET Saturated**

$$I_G = 6.6/100 = 66\text{mA}$$

$$t = \frac{(\text{curve divisions}) \times I_T \mu\text{s}}{66} = \frac{8}{66} = 121\text{ns}$$

Figure 11 shows RFM15N15 waveforms using the conditions specified in the example.

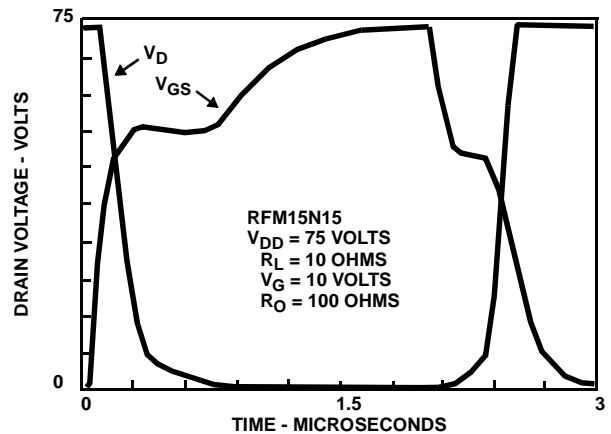


FIGURE 11. STEP GATE VOLTAGE INPUT TO AN RFM15N15

STATE	CALCULATED TIME	MEASURED TIME	RATIO
	( $t_C$ , ns)	( $t_M$ , ns)	( $t_C/t_M$ )
1	61	60	1.02
2 + 3	617	670	0.92
4	125	137	0.91
5 + 6	271	375	0.72

For peak gate voltages other than 10 volts, and load resistances other than  $BV_{DSS}/I_{D(MAX)}$ , the equations of Table 1 may be used in conjunction with slope estimates from the characterization curves for  $C_X$  and  $C_{GS} + C_X(1 + g_M/g_{MJ})$  at the appropriate drain-current level.

## Characterization-Curve Limits

The switching-time range over which the characterization can be applied is very impressive. For gate currents of the order of microamperes, device dissipation is the limiting factor. For gate currents of the order of amperes, the device response will be slowed by gate propagation delay. This delay, of course, degrades the linear switching relationship to gate current. However, as Figure 12 graphically shows, the characterization is valid across five decades of gate current and switching time, allowing all but a very few switching applications to be described by the characterization curves of Figure 9.

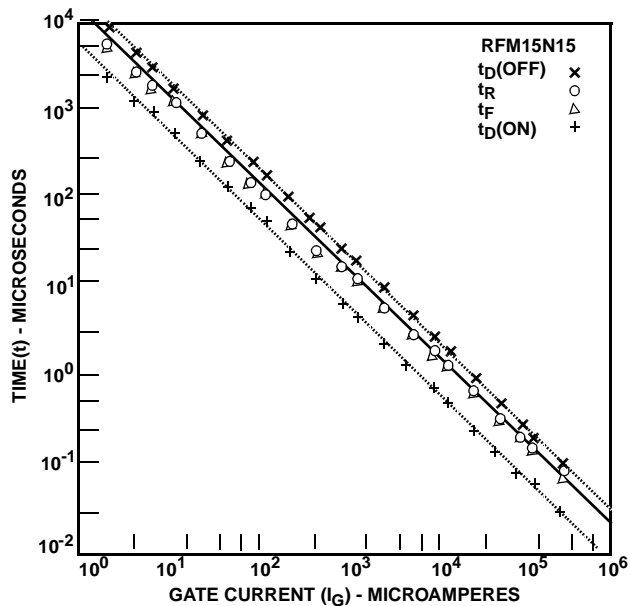


FIGURE 12. FIVE DECADES OF LINEAR RESPONSE

## Conclusions

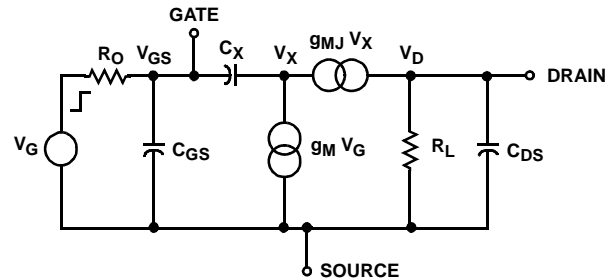
The viability of the proposed characterization curves using constant current has been demonstrated and the limits of application defined. The existence of a vertical JFET in a power MOSFET makes data-sheet capacitances of little use for estimating switching times. The classical method of defining switching time by 10% and 90% is a poor representation for power MOSFETs because of the dual-slope nature of the drain waveforms. Switching influences are masked because the 10% level is controlled by one mechanism and the 90% level by another. Device comparisons based on the classical switching definition can be very misleading.

## Appendix A - Analysis for Resistive Step Voltage Inputs

### Step Voltage Gate Drive

To obtain the necessary relationships, six device switching

states must be examined using the same device equivalent circuit as was used for the constant-gate-current case, but with the forcing function replaced with a step voltage with internal resistance  $R_O$ , Figure A-1.



### LEGEND

$V_{GS}$	- Gate Voltage	$C_{DS}$	- Drain Source Capacitance
$V_X$	- JFET Driving Voltage	$g_M$	- MOSFET Transconductance
$V_D$	- Drain Voltage	$g_{MJ}$	- JFET Transconductance
$C_{GS}$	- Gate Source Capacitance	$R_L$	- Drain Load Resistance
$C_X$	- MOSFET Feedback Capacitance	$I_G$	- Constant Current Amplitude

FIGURE A-1. POWER MOSFET EQUIVALENT CIRCUIT

### State 1: Mos Off, JFET Off

As before, both current generators are open circuits, reducing the equivalent circuit to simply charging  $C_{ISS}$  through  $R_O$ .

$$t = R_O C_{ISS} \ln(1/(1 - V_{GS(TH)}/V_G))$$

### State 2: Mos Active, JFET Active

Before proceeding, it is wise to examine an actual device response and make use of available simplifications. Figure A-2 shows  $i_G(t)$  and  $i_D(t)$  for a typical power MOSFET driven by a step gate voltage. For truly resistive switching, realize that these waveforms are only mirror images of their voltage counterparts  $v_G(t)$  and  $v_D(t)$ . Using Figure A-2, applicable gate currents for each of the device states may be listed.

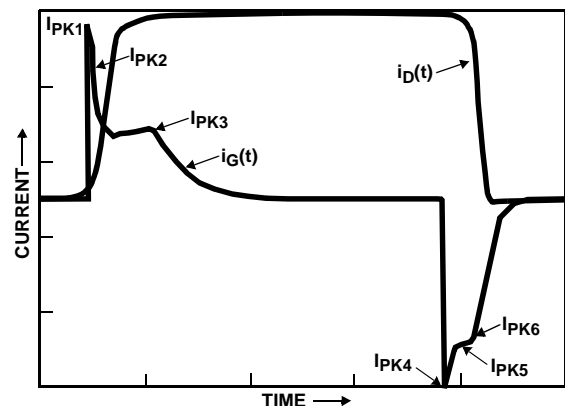


FIGURE A-2.  $i_G(t)$  AND  $i_D(t)$  FOR A TYPICAL POWER MOSFET DRIVEN BY A STEP GATE VOLTAGE

## Turn-On

### State 1: MOS Off, JFET Off

$$I_{PK1} = V_G/R_O$$

### State 2: MOS Active, JFET Active

$$I_{PK2} = (V_G - V_{GS(TH)})/R_O$$

### State 3: MOS Active, JFET Saturated

$$I_{PK3} = (V_G - V_{G(SAT)})/R_O$$

## Turn-Off

### State 4: MOS Saturated, JFET Saturated

$$I_{PK4} = V_G/R_O$$

### State 5: MOS Active, JFET Saturated

$$I_{PK5} = V_{G(SAT)}/R_O$$

### State 6: MOS Active, JFET Active

$$I_{PK6} = V_{G(SAT)}/R_O$$

The equivalent circuit of Figure A-1 predicts that:

$$dV_D/dt = (-g_M R_L (V_G - V_{GS(TH)}) e^{-t/T1}) / T1$$

where  $T1 = R_O C_{GS} + (1 + g_M/g_{MJ}) R_O C_X$

Note that  $g_M R_L (V_G - V_{GS(TH)})$  is usually an order of magnitude greater than  $V_{DD}$ , indicating that the drain voltage is discharging toward a very large negative value. The device operation, then, is on the early, almost linear, portion of the exponential, where  $e^{-t/T1}$  approximates unity. The drain current of Figure A-2, and hence the drain voltage, does indeed exhibit a linear decrease with time.

Thus, for state 2:

$$t = \frac{[V_{DD} - V_{DK}] [C_{GS} + C_X (1 + g_M/g_{MJ})]}{g_M R_L I_{PK2}}$$

where  $I_{PK2} = (V_G - V_{GS(TH)})/R_O$

### State 3: Mos Active, JFET Saturated

Because of the Miller effect, the gate voltage and, hence, the gate current, is almost constant during the tail time. The equivalent circuit then predicts:

$$\frac{dV_D}{dt} = \frac{g_M R_L I_G}{C_{GS} + (1 + g_M R_L) C_X} = \frac{I_G}{C_X}$$

$$I_G = I_{PK3} = (V_G - V_{G(SAT)})/R_O$$

$$\text{and } t = \frac{(V_{DK} - V_{D(SAT)}) C_X}{I_{PK3}}$$

### State 4: Mos Saturated, JFET Saturated (Turn-off)

Both equivalent-circuit generators are short circuits, and the gate drive is discharging  $C_X$  in parallel with  $C_{GS}$  through  $R_O$ .

$$t = R_O (C_{GS} + C_X) \ln[V_G/V_{G(SAT)}]$$

$$I_{PK4} = V_G/R_O$$

### State 5: Mos Active, JFET Saturated

The JFET current generator  $V_X g_{mJ}$ , is operative.

$$t = \frac{[V_{DK} - V_{D(SAT)}) C_X}{I_{PK5}}$$

$$I_{PK5} = V_{G(SAT)}/R_O$$

### State 6: Mos Active, JFET Active

The Miller effect is now reduced by the activation of  $V_{G9MJ}$ , and the equivalent circuit predicts:

$$t = \frac{[V_{DD} - V_{DK}] [C_{GS} + C_X (1 + g_M/g_{MJ})]}{g_M R_L I_{PAK6}}$$

$$I_{PAK6} = V_{G(SAT)}/R_O$$

## Appendix B - Estimating $R_O$ for Some Typical Gate-Drive Circuits

### Case 1: Typical Pulse-Generator Drive, Figure B-1

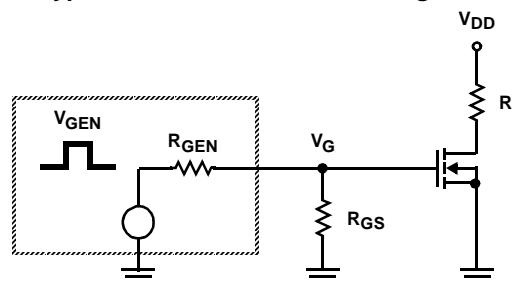


FIGURE B-1. TYPICAL PULSE-GENERATOR DRIVE CIRCUIT

#### Turn-On and Turn-Off

$$R_O = R_{GEN} R_{GS} / (R_{GEN} + R_{GS})$$

For the typical case where  $R_{GEN} = 50\Omega$ , and a coaxial-cable termination of 50 ohms,  $R_O = 25\Omega$  and  $V_G = V_{GEN}/2$ .

### Case 2: Voltage-Follower Gate Drive, Figure B-2

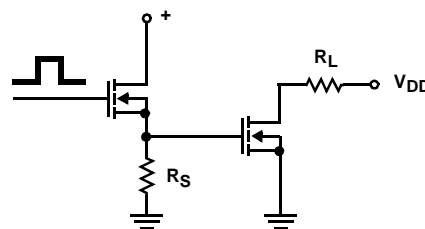


FIGURE B-2. VOLTAGE-FOLLOWER GATE-DRIVE CIRCUIT

#### Turn-On

$R_O$  is approximately equal to  $1/g_M$  for  $R_S$  very much greater than  $1/g_M$ .

$g_M$  = transconductance of driving MOSFET transistor.

#### Turn Off

$$R_O = R_S$$

## Case 3 :Common-Source Gate Drive, Figure B-3

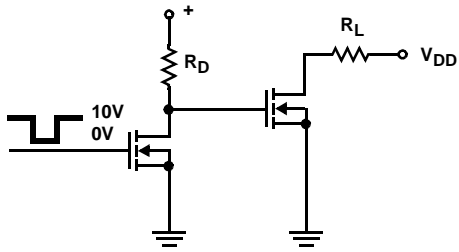


FIGURE B-3. COMMON-SOURCE GATE-DRIVE CIRCUIT

### Turn-On

$$R_O = R_D$$

(drain-to-ground capacitance of driving device adds to  $C_{GS}$  of driven MOSFET.)

### Turn Off

$R_O = r_{DS(ON)}$  of driving MOSFET when

$R_D$  is very much greater than  $R_{DS(ON)}$



## TRADEMARKS

The following are registered and unregistered trademarks Fairchild Semiconductor owns or is authorized to use and is not intended to be an exhaustive list of all such trademarks.

ACE <sub>x</sub> <sup>™</sup>	FAST <sup>®</sup>	MICROWIRE <sup>™</sup>	SILENT SWITCHER <sup>®</sup>	UHC <sup>™</sup>
Bottomless <sup>™</sup>	FAST <sub>r</sub> <sup>™</sup>	OPTOLOGIC <sup>®</sup>	SMART START <sup>™</sup>	UltraFET <sup>®</sup>
CoolFET <sup>™</sup>	FRFET <sup>™</sup>	OPTOPLANAR <sup>™</sup>	SPM <sup>™</sup>	VCX <sup>™</sup>
CROSSVOLT <sup>™</sup>	GlobalOptoisolator <sup>™</sup>	PACMAN <sup>™</sup>	STAR*POWER <sup>™</sup>	
DenseTrench <sup>™</sup>	GTO <sup>™</sup>	POP <sup>™</sup>	Stealth <sup>™</sup>	
DOME <sup>™</sup>	HiSeC <sup>™</sup>	Power247 <sup>™</sup>	SuperSOT <sup>™</sup> -3	
EcoSPARK <sup>™</sup>	I <sup>2</sup> C <sup>™</sup>	PowerTrench <sup>®</sup>	SuperSOT <sup>™</sup> -6	
E <sup>2</sup> CMOS <sup>™</sup>	ISOPLANAR <sup>™</sup>	QFET <sup>™</sup>	SuperSOT <sup>™</sup> -8	
EnSigna <sup>™</sup>	LittleFET <sup>™</sup>	QS <sup>™</sup>	SyncFET <sup>™</sup>	
FACT <sup>™</sup>	MicroFET <sup>™</sup>	QT Optoelectronics <sup>™</sup>	TinyLogic <sup>™</sup>	
FACT Quiet Series <sup>™</sup>	MicroPak <sup>™</sup>	Quiet Series <sup>™</sup>	TruTranslation <sup>™</sup>	

STAR\*POWER is used under license

## DISCLAIMER

FAIRCHILD SEMICONDUCTOR RESERVES THE RIGHT TO MAKE CHANGES WITHOUT FURTHER NOTICE TO ANY PRODUCTS HEREIN TO IMPROVE RELIABILITY, FUNCTION OR DESIGN. FAIRCHILD DOES NOT ASSUME ANY LIABILITY ARISING OUT OF THE APPLICATION OR USE OF ANY PRODUCT OR CIRCUIT DESCRIBED HEREIN; NEITHER DOES IT CONVEY ANY LICENSE UNDER ITS PATENT RIGHTS, NOR THE RIGHTS OF OTHERS.

## LIFE SUPPORT POLICY

FAIRCHILD'S PRODUCTS ARE NOT AUTHORIZED FOR USE AS CRITICAL COMPONENTS IN LIFE SUPPORT DEVICES OR SYSTEMS WITHOUT THE EXPRESS WRITTEN APPROVAL OF FAIRCHILD SEMICONDUCTOR CORPORATION.

As used herein:

1. Life support devices or systems are devices or systems which, (a) are intended for surgical implant into the body, or (b) support or sustain life, or (c) whose failure to perform when properly used in accordance with instructions for use provided in the labeling, can be reasonably expected to result in significant injury to the user.
2. A critical component is any component of a life support device or system whose failure to perform can be reasonably expected to cause the failure of the life support device or system, or to affect its safety or effectiveness.

## PRODUCT STATUS DEFINITIONS

### Definition of Terms

Datasheet Identification	Product Status	Definition
Advance Information	Formative or In Design	This datasheet contains the design specifications for product development. Specifications may change in any manner without notice.
Preliminary	First Production	This datasheet contains preliminary data, and supplementary data will be published at a later date. Fairchild Semiconductor reserves the right to make changes at any time without notice in order to improve design.
No Identification Needed	Full Production	This datasheet contains final specifications. Fairchild Semiconductor reserves the right to make changes at any time without notice in order to improve design.
Obsolete	Not In Production	This datasheet contains specifications on a product that has been discontinued by Fairchild semiconductor. The datasheet is printed for reference information only.

Rev. H5

## Free Manuals Download Website

<http://myh66.com>

<http://usermanuals.us>

<http://www.somanuals.com>

<http://www.4manuals.cc>

<http://www.manual-lib.com>

<http://www.404manual.com>

<http://www.luxmanual.com>

<http://aubethermostatmanual.com>

Golf course search by state

<http://golfingnear.com>

Email search by domain

<http://emailbydomain.com>

Auto manuals search

<http://auto.somanuals.com>

TV manuals search

<http://tv.somanuals.com>